Available online at www.sciencedirect.com
ScienceDirect
Comput. Methods Appl. Mech. Engrg. 282 (2014) 71–86
Computer methods in applied mechanics and engineering
www.elsevier.com/locate/cma

An explicit length scale control approach in SIMP-based topology optimization

Weisheng Zhang, Wenliang Zhong, Xu Guo*

State Key Laboratory of Structural Analysis for Industrial Equipment, Department of Engineering Mechanics, Dalian University of Technology, Dalian, 116023, PR China

Received 10 June 2014; received in revised form 5 August 2014; accepted 27 August 2014
Available online 8 September 2014

Abstract

The present paper aims to present a new approach for controlling both maximum and minimum length scales of structural members in the Solid Isotropic Material with Penalization (SIMP)-based topology optimization framework. In the proposed approach, length scale control is achieved with help of structural skeleton, which is a key concept in mathematical morphology and a powerful tool for describing structural topologies. Numerical examples show that the proposed approach does have the capability to give a complete control of the length scales of an optimal structure in an explicit and local way.

Keywords: Topology optimization; Length scale control; SIMP; Structural skeleton

1. Introduction

Since the pioneering work of Bendsoe and Kikuchi [1], topology optimization, which aims at distributing available material in a prescribed design domain in an optimal way, has undergone tremendous development. Nowadays, topology optimization has been used successfully in many industrial fields, such as automotive, aerospace and so on. A state-of-the-art review and some recent developments in this field can be found in the review articles [2–4] and the references therein.

Although remarkable achievements have been made in the field of topology optimization, there still exist some challenging issues which need to be further addressed. One of them is how to control the length scales (i.e., minimum/maximum feature sizes) of structural members in topology optimization. The importance of length scale control consists in the fact that without considering this issue, the obtained optimal topology designs may be unmanufacturable (e.g., existence of holes with very small radii) or very fragile with respect to some specific loading cases (e.g., existence of very slender bars which will buckle under slight compression).

A lot of efforts have been devoted to the development of topology optimization approaches that can handle the issue of length scale control. The pioneering work can be traced back to [5], where a so-called sensitivity filter scheme

* Corresponding author. Tel.: +86 411 84707807.
E-mail address: guoxu@dlut.edu.cn (X. Guo).

http://dx.doi.org/10.1016/j.cma.2014.08.027
0045-7825/

to eliminate mesh-dependent results and checkerboard patterns was suggested. In their paper, it was shown that the proposed approach also had the ability to control the minimum length scale in the structure implicitly. Later on, Petersson et al. [6] found that the slope-constrained formulation also had the effect of minimum length scale control for optimal structural topology. Poulsen proposed a so-called MOLE (MOnotonicity based minimum LEngth scale) method for achieving the minimum length scale in topology optimization [7]. The key idea is to introduce a global functional $L(\boldsymbol{\rho}, d)$ which can measure the magnitude of variations of density field (i.e., $\boldsymbol{\rho}$) along specific directions within some prescribed length scale. It can be proved theoretically that minimum length scale d can be controlled by letting $L(\boldsymbol{\rho}, d) \leq 0$. Guest et al. suggested a very effective minimum length scale control approach for topology optimization by using nodal values of density field as primary design variables [8]. In this approach, a projection operator is introduced to project the nodal values of density field onto the element space to determine the element density used for stiffness interpolation. In this way, the size of the support set of the weight function appeared in the projection operator can be used to control the minimum allowable length scale in the optimal topology implicitly. Guest also developed a scheme for imposing maximum length scale in topology optimization [9]. In this approach, the radius of the circular test region serves as the value that determines the maximum allowable member size in the optimized structures. It is worth noting that all of the above treatments are based on the SIMP framework.

Research works on length scale control in topology optimization have also been carried out in level set-based framework. For example, Zhu and Zhang suggested a strain energy based approach to impose the minimum length scale constraint implicitly [10]. Chen et al. introduced a quadratic energy functional into topology optimization formulation for length control [11]. Luo et al. also adopted the same idea to the design of hinge-free compliant mechanisms [12]. More recently, Guo et al. proposed a level set-based approach for feature control in optimal topology designs [13]. In their work, medial surface and signed distance function have been used to give precise definitions of the minimum and maximum length scales of a structure. Based on these definitions, corresponding problem formulation and numerical schemes that can control the maximum/minimum length scales locally and explicitly are developed. Furthermore, it was also found that implicit minimum length scale control can also be achieved by resorting to the wavelet-based methods [14,15] and robust topology optimization formulations [16–18].

Although a lot of research efforts have been devoted to the length scale control in topology optimization, it has not reached a mature stage up to now. For example, the sensitivity filter and slope-constrained approaches suffer from the undesirable boundary diffusion effect (i.e., existence of gray elements along the boundary of the structure). Guest's projection scheme also has the same problem. Although almost 0–1 designs can be obtained by post-processing techniques, the corresponding computational efforts are not negligible. Furthermore, these methods can only be used to control the minimum length scale of the structure. The common problem associated with Guest's maximum length scale control approach and Poulsen's minimum length scale control approach is that a large number of nonlinear constraints are involved in the problem formulation. This may render the corresponding numerical treatment intractable if the resulting optimization problems are solved directly. Chen et al.'s method seems tough for numerical implementation since a non-local energy term involving double layer boundary integral must be handled. It can only control the length scale in an implicit way. Although Guo et al.'s approach can control the minimum and maximum length scales simultaneously, it is only applicable in the level set-based topology optimization framework. As pointed in [19], the development of more efficient *local* and *explicit* length scale control approaches especially in the SIMP framework, which is the most versatile framework for topology optimization, is still much needed.

In the present paper, we intend to discuss how to carry out local and explicit length scale control in structural topology optimization under SIMP-based computational framework. This is achieved by introducing some new length scale measures into the problem formulation with which the size of the structure members can be controlled effectively. The rest of the paper is organized as follows. In Section 2, some basic ideas depending on mathematical morphology are explained. Then the considered problem is presented in Section 3. In Section 4, numerical solution aspects are discussed. Some numerical examples are presented in Section 5 to illustrate the effectiveness of the proposed approach. Finally some concluding remarks are given in the last section.

2. Structural skeleton and the definitions of minimum/maximum length scales of a structure

In order to give a precise length control of a structure, it is necessary to define the minimum/maximum length scales in a mathematical rigorous way. In the following, this will be achieved by introducing the concept of structural skeleton of a given structure. The structural skeleton of a structure occupying a region Ω, that is $\mathcal{SS}(\Omega)$ is constituted

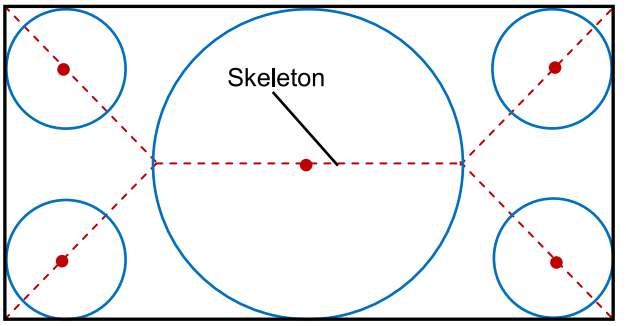

Fig. 1. Schematic illustration of the concept of structural skeleton.

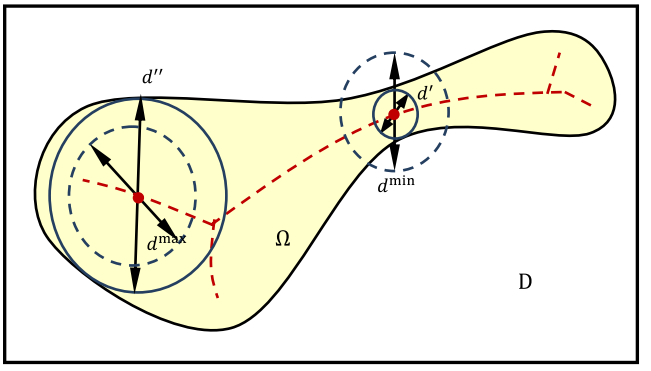

Fig. 2. Schematic illustration of the minimum and maximum length scale constraints.

by the points which have at least two closest points on $\partial\Omega$-the boundary of Ω. In other word, $\mathbb{SS}(\Omega)$ is the set of all centers of the closed maximal balls (see Fig. 1 for reference). With use of the concept of structural skeleton, the length scale of a structure can be defined in the following form:

Definition 1. The minimum/maximum length scale of a structure.

Suppose that Ω is a closed domain in R^3 and $\mathbb{SS}(\Omega)$ is its structural skeleton. Then the minimum length scale $d^{\min}(\Omega)$ and maximum length scale $d^{\max}(\Omega)$ of Ω can be defined as

$$d^{\min}(\Omega) = \inf_{\boldsymbol{x}\in\mathbb{SS}(\Omega)} D(\boldsymbol{x}) \tag{2.1a}$$

and

$$d^{\max}(\Omega) = \sup_{\boldsymbol{x}\in\mathbb{SS}(\Omega)} D(\boldsymbol{x}), \tag{2.1b}$$

respectively, where $D(\boldsymbol{x})$ is defined as

$$D(\boldsymbol{x}) = \sup_{r\geq 0}\{2r \mid \mathcal{B}(\boldsymbol{x}, r) \subseteq \Omega\}, \quad \text{for } \forall \boldsymbol{x} \in \mathbb{SS}(\Omega). \tag{2.2}$$

In Eq. (2.2), $\mathcal{B}(\boldsymbol{x}, r)$ denotes a closed ball centered at $\boldsymbol{x}$ with radius r. Suppose that the lower and upper bound of the length scale are $\underline{d}$ and $\overline{d}$, respectively. Obviously, if there exists some point $\tilde{\boldsymbol{x}} \in \mathbb{SS}(\Omega)$, $d' \in D(\tilde{\boldsymbol{x}})$ such that $d' \leq \underline{d}$, then the corresponding minimum length scale constraint $d^{\min}(\Omega) \geq \underline{d}$ will be violated. Similarly, if there exists some point $\tilde{\boldsymbol{x}} \in \mathbb{SS}(\Omega)$, $d'' \in D(\tilde{\boldsymbol{x}})$ such that $d'' \geq \overline{d}$, then it implies that the inequality $d^{\max}(\Omega) \leq \overline{d}$ does not hold. The above definitions are illustrated in Fig. 2.

If the topology of a structure can be represented by a binary bitmap, numerous well established image processing techniques can be employed to extract its skeleton. In the present work, the straight skeleton algorithm [20] is adopted. See Section 4 for more discussions.

3. Problem statement and formulation

In present work, the topology optimization problem under consideration is to minimize the structural compliance under available volume and minimum/maximum length scale constraints. In the SIMP framework, the optimization problem can be formulated as follows:

$$
\begin{aligned}
&\text{Find } \boldsymbol{\rho} = (\rho_1, \rho_2, \ldots, \rho_n)^{\top}, \boldsymbol{u} \\
&\text{Min } C = \boldsymbol{u}^{\mathsf{T}} \boldsymbol{K}(\boldsymbol{\rho})\, \boldsymbol{u} \\
&\text{s.t.} \\
&\boldsymbol{K}(\boldsymbol{\rho})\, \boldsymbol{u} = \boldsymbol{f}, \\
&V(\boldsymbol{\rho}) = \sum_{i=1}^{n} \rho_i v_i \Big/ \sum_{i=1}^{n} v_i \le \bar{V}, \\
&g_1(\boldsymbol{\rho}) = \sum_{j \in I_{\min}} \left(\rho_j - 1\right)^2 \le \epsilon_1, \\
&g_2(\boldsymbol{\rho}) = \sum_{k \in I_{\max}} \left(\rho_k - \rho_{\min}\right)^2 \le \epsilon_2, \\
&\rho_{\min} \le \rho_i \le 1, \quad \forall i = 1, \ldots, n.
\end{aligned}
\tag{3.1}
$$

In Eq. (3.1), $\boldsymbol{\rho}$ is the vector of the design variables with ρ_i and v_i denoting the density and volume of the ith element. The symbol n denotes the total number of finite element used for discretizing the prescribed design domain D. $\boldsymbol{K} = \sum_{i=1}^{n} \rho_i^p \boldsymbol{K_0}$ (p is the penalization index and $p = 3$ is adopted in the present study) is the global stiffness matrix with $\boldsymbol{K_0}$ representing the element stiffness matrix corresponding to $\rho_i = 1$. $\rho_{\min}$ is the lower bound of the element density. $g_1 \le \epsilon_1$ and $g_2 \le \epsilon_2$ are the minimum and maximum length scale constraint, respectively. $\bar{V}$ is the prescribed upper bound of the solid material. $\boldsymbol{f}$ and $\boldsymbol{u}$ are the external load and the displacement field, respectively. In Eq. (3.1), $I_{\min}$ and $I_{\max}$ are two index sets such that

$$
I_{\min} = \left\{ j \,|\, j \in \{1, \ldots, n\},\, \Omega_j \in \bigcup_{\boldsymbol{x} \in \mathcal{SS}(\Omega)} \mathcal{B}\left(\boldsymbol{x}, \underline{d}\right) \right\}, \tag{3.2a}
$$

and

$$
I_{\max} = \left\{ k \,|\, k \in \{1, \ldots, n\},\, \Omega_k \notin \bigcup_{\boldsymbol{x} \in \mathcal{SS}(\Omega)} \mathcal{B}\left(\boldsymbol{x}, \overline{d}\right) \right\}, \tag{3.2b}
$$

respectively (see Fig. 3 for reference). In Eq. (3.2), Ω_j and Ω_k denote the region occupied by the jth and kth element, respectively. It is obvious that $g_1 \le \epsilon_1$ and $g_2 \le \epsilon_2$ imply $d^{\min}(\Omega) \ge \underline{d}$ and $d^{\max}(\Omega) \le \overline{d}$ when $\epsilon_1 \to 0$ and $\epsilon_2 \to 0$. Numerical examples presented in Section 5 indicate that the above problem formulation can give a local and explicit control of the minimum and maximum length scale of the optimized structure.

4. Numerical solution aspects

In this section, some numerical solution aspects of the proposed approach for length scale control in topology optimization are discussed in detail.

4.1. The identification of structural skeleton

As discussed in the above section, the identification of the structural skeleton (i.e., $\mathcal{SS}(\Omega)$) plays the essential role in the proposed approach for length control. However, the well-established image processing techniques for extracting the skeleton from a binary bitmap cannot be applied directly to the considered problem since gray elements will inevitably appear during the course of topology optimization. Taking this fact into consideration, we propose to

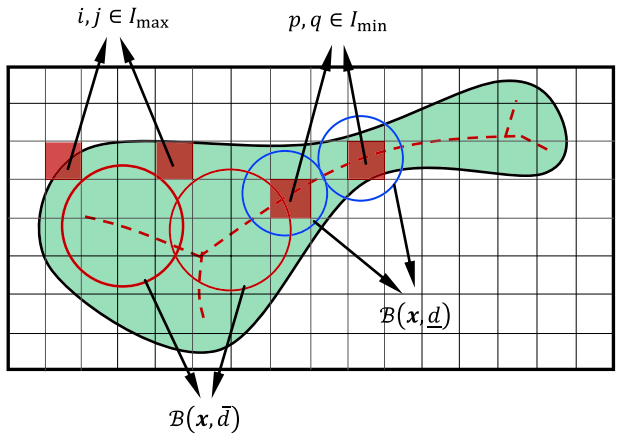

Fig. 3. Schematic illustration of the index sets $I_{\min}$ and $I_{\max}$ respectively.

introduce the following projection operator to transform the gray-valued density field (i.e., $\rho(\boldsymbol{x})$) into a pure black-and-white density field (i.e., $\hat{\rho}(\boldsymbol{x})$) used for extracting the structural skeleton:

$$\hat{\rho}(\boldsymbol{x}) = \begin{cases} 1, & \text{if } \rho(\boldsymbol{x}) \geq \bar{\rho}, \\ 0, & \text{otherwise}, \end{cases} \tag{4.1}$$

where $\bar{\rho}$ is a threshold value for density projection. In the present work, we will make use of Otsu method [21] to determine $\bar{\rho}$ in every optimization step adaptively in order to avoid misrecognition. Once the binary density field is identified, the iterative skeleton algorithm [22,23] can be adopted to identify the structural skeleton. For the sake of completeness, the basic ideas of this algorithm will be explained as follows. Let $\mathcal{L}$ denote the binary density representation, for a specified pixel $p \in \mathcal{L}$, we can construct a pattern P of p by collecting all its 8-neighbors, as shown in Fig. 4(a). If the removal of p does not change the connectivity of P, then pixel p can be denoted as a deletable pixel, otherwise, p is a retainable pixel (see Fig. 4(b) and (c) for reference). For some special points, such as final point and contour point (see Fig. 4(d) and (e) for reference), we can make use of the following crossing number indicator to determine the deletability of p:

$$X_R(p) = \sum_{i=1}^{8} |x_{i+1} - x_i|, \tag{4.2}$$

where $x_9 = x_1$. If $X_R(p) = 0$ or 8, then p is a retainable point. For more detailed discussions about the complete conditions, we refer the readers to [24].

Following the above instructions, all pixels can be detected as deletable or retainable by searching the whole set of $\mathcal{L}$, and all deletable pixels are then removed. In present work, this scan operation is carried out only for the pixels where $p = 1$, since only the skeletons of solid material are focused on. The produce will be repeated until no pixels can be removed any more and the retained pixels constitute the set of $\mathcal{SS}(\Omega)$ which is the skeleton of the structure. We refer the readers to Fig. 4(f) for a schematic illustration of the above iterative procedure. It is also worth noting that in the present numerical implementation, the extraction of the structural skeleton is achieved by calling the MATLAB function BW2 = bwmorph (BW1, OPERATION, N), where BW1 is a input binary image, OPERATION indicates the type of skeleton (OPERATION = skel is adopted in the present work), N denotes the maximum number of iteration (N = inf is adopted in the present work) and BW2 is the output skeleton of BW1, respectively.

4.2. Sensitivity analysis

In order to obtain mesh-independent and black-and-white topology optimization results, numerous approaches have been suggested. Among them, the sensitivity filter approach proposed by Sigmund [5] is the most efficient one for suppressing the numerical instabilities in SIMP-based topology optimization. The original form of the sensitivity

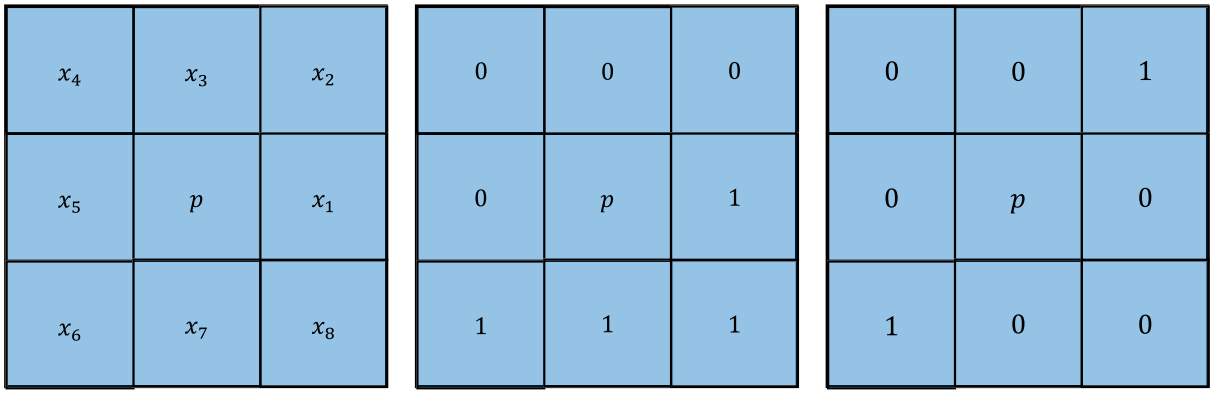

(a) Schematic illustration of a pixel p and its 8 neighbors.

(b) A pixel p is deletable.

(c) An interior pixel p is retainable.

(d) A contour pixel is retainable.

(e) An end pixel is retainable.

Fig. 4. Schematic illustration of the iterative skeleton algorithm.

filter scheme is as follows:

$$\frac{\hat{\partial} l}{\partial \rho_k} = \frac{1}{\rho_k \sum_{i=1}^{N} \hat{H}_i} \sum_{i=1}^{N} \hat{H}_i \rho_i \frac{\partial l}{\partial \rho_i}, \tag{4.3}$$

where $\hat{\partial} l / \partial \rho_k$ and $\partial l / \partial \rho_i$ are the filtered and unfiltered sensitivities of the concerned objective/constraint functional l (for the considered problem, l is the structural compliance). The symbols ρ_k and ρ_i denote the densities of the considered kth element and the ith element contained in the filter region of element k. N is the total number of elements in the spherical filter region with radius R. The weight factor $\hat{H}_i$ is defined as

$$\hat{H}_i = R - dist\,(i,k)\,, \quad \forall i \text{ such that } dist\,(i,k) \leq R, \tag{4.4}$$

where $dist\,(i,k)$ is the distance between the centers of element i and k. Although powerful enough, a side effect of the filter scheme in Eq. (4.3) is that it will inevitably induce a density transition region along the structural boundary (i.e., boundary diffusion). In order to alleviate the boundary diffusion effect caused by the original version of the sensitivity filter approach, here, we propose a modified filter scheme in the following form:

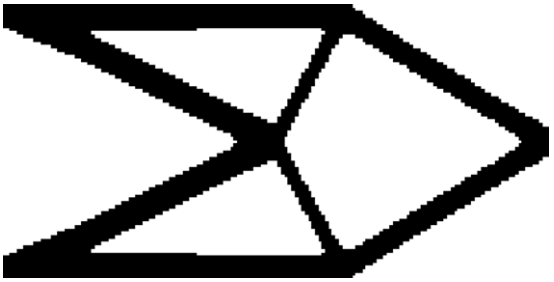

Initial binary bitmap

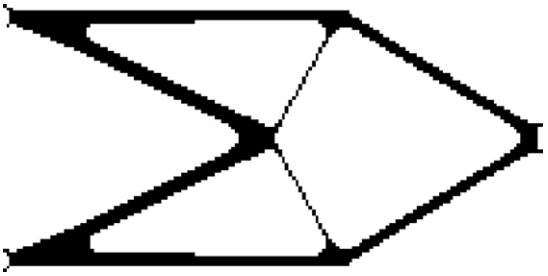

Intermediate identification step

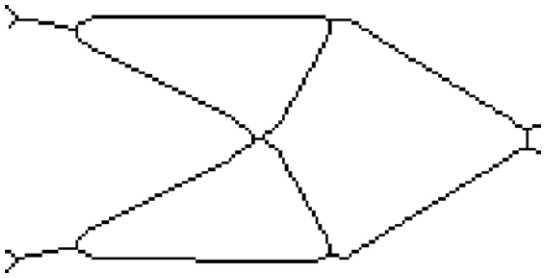

Identified structural skeleton

(f) Iteration of skeleton identification.

Fig. 4. (*continued*)

$$\frac{\partial \hat{l}}{\partial \rho_k} = \frac{1}{(\rho_k)^{\eta} + \left(\sum_{j=1}^{4} \rho_j\right)^{\nu}} \frac{\sum_{i=1}^{N} \hat{H}_i \, (\rho_i)^{\gamma} \, \frac{\partial l}{\partial \rho_i}}{\sum_{i=1}^{N} \hat{H}_i}, \tag{4.5}$$

where $0 < \eta < 1$, $\gamma \geq 1$ and $0 < \nu < 1$ are three adjustable parameters. In Eq. (4.5), the summation in $\sum_{j=1}^{4} \rho_j$ is taken for the four second-nearest neighborhood elements around element k. Numerical experiments show that the above filter scheme is effective to eliminate gray elements along the structural boundary and therefore can obtain much improved black-and-white designs.

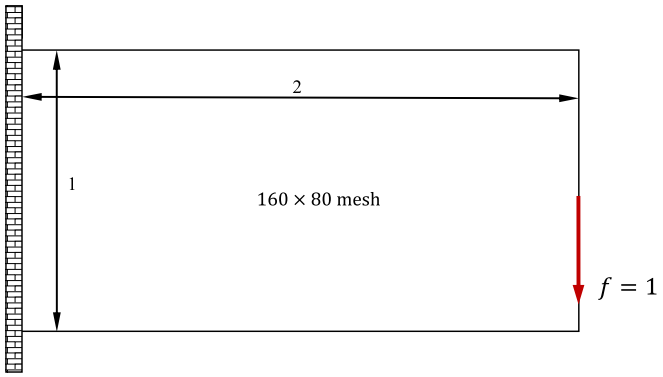

Fig. 5a. The design domain of the short beam example.

By assuming that the index sets $I_{\min}$ and $I_{\max}$, do not change before and after the perturbations of design variables, it holds that $\partial g_1/\partial \rho_j = 2\left(\rho_j - 1\right), \forall j \in I_{\min}, \partial g_1/\partial \rho_j = 0, \forall j \notin I_{\min}$ and $\partial g_2/\partial \rho_k = 2\left(\rho_k - \rho_{\min}\right), \forall k \in I_{\max}, \partial g_2/\partial \rho_k = 0, \forall k \notin I_{\max}$ respectively.

4.3. Optimization algorithm

In present paper, the Method of Moving Asymptotes (MMA) [25] is used to update the design variables. It should be noticed that g_1 and g_2 in Eq. (3.1) are highly non-convex functions of the design variables and therefore the final optimization results are expected to be only local minima. Furthermore, in order to prevent the length scale constraints from hindering the formation of the appropriate load-carrying structural topology at initial stages of optimization, these constraints should be imposed in a soft way from numerical implementation point of view. Taking the above facts into consideration, we suggest to employ a continuation strategy to deal with the length scale constraints, that is, the values of the relaxation parameters ϵ_1 and ϵ_2 in Eq. (3.1) should be decreased continuously from relatively large values to some specific tolerance values during the course of optimization.

5. Numerical examples

In this section, several numerical examples are presented to illustrate the effectiveness of the proposed length scale control measure. For illustration purpose, the material, load and geometry data are chosen as dimensionless. Young's modulus and Poisson's ratio of the solid material are taken as $E = 1$ and $\nu = 0.3$, respectively. Four-node bilinear square elements are adopted for finite element discretization. The lower bound of the density variable is $\rho_{\min} = 10^{-2}$ in numerical implementation. Unless otherwise stated, the relaxation parameters ϵ_1 and ϵ_2 are set to be 10^2 initially and reduced to 1 within 20 iterative steps. The filter radius for regularization is chosen as $r = 1.2$. The values of the parameters η, ν and γ are chosen as 0.1, 0.05 and 2 in all tested examples, respectively.

5.1. Short beam example

In this example, the classical short beam problem shown in Fig. 5a is examined to investigate the capability of the proposed method for length scale control. The design domain is discretized by a 160×80 finite element (FEM) mesh. For comparison purpose, first the classical compliance minimization problems without length scale constraints are solved with $\bar{V} = 0.3$, $\bar{V} = 0.4$ and $\bar{V} = 0.5$, respectively. The optimal structural topologies are shown in Fig. 5b. From this figure, it is observed that the typical sizes of the structural members in optimized structures increase as the upper bound of the available material volume increases. It is worth noting that when $\bar{V} = 0.5$, the maximum length scale of the corresponding optimized structure is more than 20 times of the FEM grid size.

Next, the same problem is solved under problem formulation (3.1) with $\underline{d} = 3 \times \min\left(\Delta x, \Delta y\right)$ and $\bar{d} = 7 \times \min\left(\Delta x, \Delta y\right)$, respectively. Figs. 5c–5e show the corresponding optimal designs and the structural skeletons. When $\bar{V} = 0.3$, it can be observed clearly that the structural members close to the clamped boundary are split into two slender beams in order to satisfy the minimum length scale constraint. Additionally, some slender beams whose

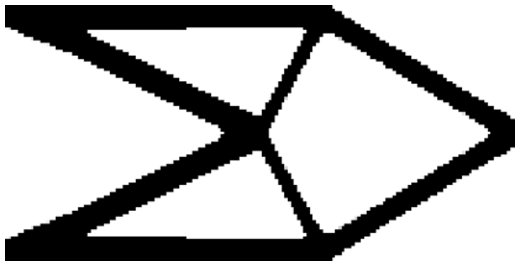

$\overline{V} = 0.3$

$\overline{V} = 0.4$

$\overline{V} = 0.5$

Fig. 5b. The optimized design of the short beam example without length scale control.

length scales are greater than $\underline{d}$ are also introduced to make the volume constraint active. This is because the structural compliance is a monotonic decreasing function of the structural volume for design independent external load. When the upper bound of volume constraint is increased, more and more slender beams grow out and the load path is more complex. It is also worth noting that introducing the maximum and minimum length scale constraints will generally degenerate the performance of the optimized structure (see Table 1 for reference). This is the price we must pay for considering the geometrical constraints.

It is worth noting that when no feature size constraint is considered, horizontal beams should be appeared in the region next to the clamped boundary in order to enhance the stiffness of the structure more efficiently. When feature size constraint is considered, however, the density changes at every iteration step of optimization are determined by the sensitivities and the current values of the objective function and the feature size constraint functions simultaneously. Basically, when the upper bound feature size constraint is violated, there are two mechanisms to improve the current design: one is bilateral material deletion while the other is unilateral material deletion with respect to the skeleton. When the upper bound feature size constraint is violated severely (this is usually the case when $\bar{d}$ is relatively small),

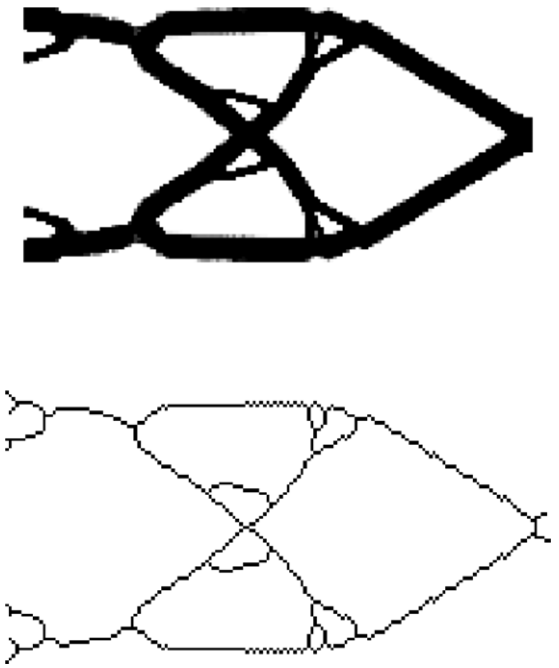

Fig. 5c. The optimized design of the short beam example with length scale control and the corresponding structural skeleton ($\bar{V} = 0.3$, $\underline{d} = 3 \times \min(\Delta x, \Delta y)$, $\bar{d} = 7 \times \min(\Delta x, \Delta y)$).

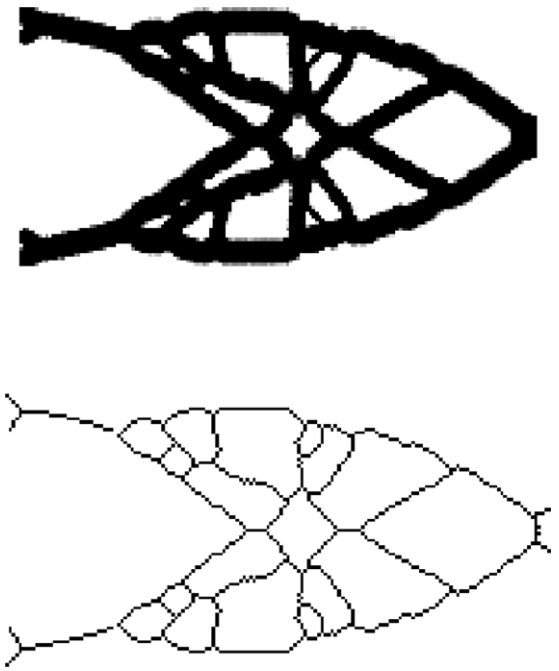

Fig. 5d. The optimized design of the short beam example with length scale control and the corresponding structural skeleton ($\bar{V} = 0.4$, $\underline{d} = 3 \times \min(\Delta x, \Delta y)$, $\bar{d} = 7 \times \min(\Delta x, \Delta y)$).

it seems that the bilateral material deletion is the more effective way to alleviate the constraint violation. If this is the case and the material deletion is not uniform along the direction of skeleton, inclined beams as shown in Fig. 5c will appear. If the appearance of this kind of inclined beams is at the final stage of iteration, it will be retained in the final optimized structure.

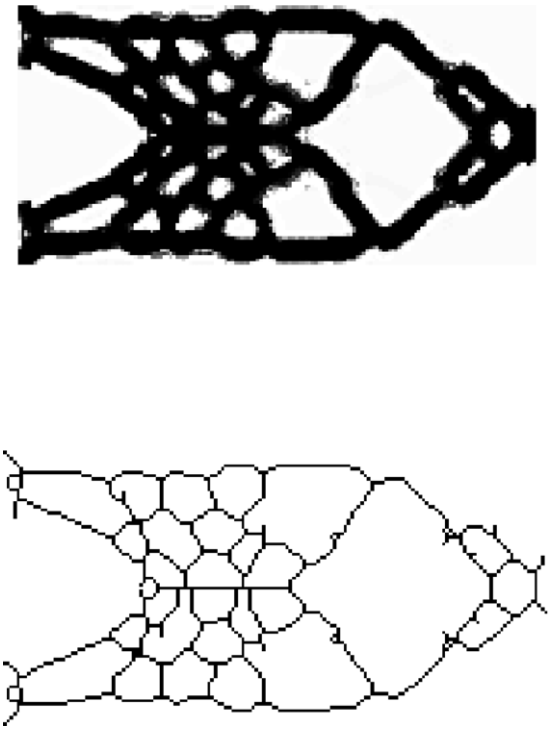

Fig. 5e. The optimized design of the short beam example with length scale control and the corresponding structural skeleton ($\bar{V} = 0.5$, $\underline{d} = 3 \times \min(\Delta x, \Delta y)$, $\bar{d} = 7 \times \min(\Delta x, \Delta y)$).

Table 1
Optimization results for the short beam problem.

Compliance $\underline{d} = 0$ $\bar{d} = +\infty$	Compliance $\underline{d} = 3 \times \min(\Delta x, \Delta y)$ $\bar{d} = 7 \times \min(\Delta x, \Delta y)$	Volume
104.82	128.52	0.3
78.65	117.28	0.4
65.26	104.80	0.5

Furthermore, in order to illustrate the robustness of the presented approach, the same problem is also solved with use of a refined FEM mesh (i.e., 240×120) and $\bar{V} = 0.3$. In order make a comparison under the same upper/lower bound of the structural feature size, we set $\underline{d} = 4.5 \times \min(\Delta x, \Delta y)$ and $\bar{d} = 10.5 \times \min(\Delta x, \Delta y)$, respectively, for the refined FEM mesh. The optimized structure obtained under refined finite element mesh is shown in Fig. 5f. It can be observed from Figs. 5c and 5f that the optimal structural topologies obtained under coarse and refined meshes are almost identical. This demonstrates clearly the mesh-independence of the proposed approach.

5.2. Compliant mechanism example

In this example, the compliant inverter problem depicted in Fig. 6a is investigated under minimum length scale constraint. The design domain is a 2×1 rectangular sheet discretized with a 100×100 FEM mesh. The left-upper and left-lower sides of the design domain are clamped as shown in Fig. 6b. Taking the symmetry property of this example into consideration, only lower half of the design domain is optimized. As suggested in [26], the displacement in the negative direction at the output point is chosen as the objective to maximize. The elastic constant of the artificial spring are $K_{in} = 0.1$ and $K_{out} = 0.1$, respectively. The actuation force applied at the left-upper point in positive direction is $f_{in} = 0.1$. First the considered problem is solved with $\bar{V} = 0.3$. It can be observed from Fig. 6b that the optimized structure has a hinge which is important to enhance the GA (Geometric Advantage) of this compliant mechanism. In

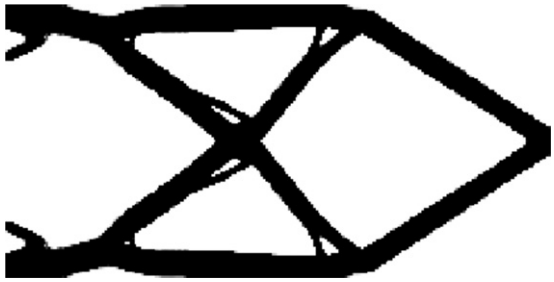

Fig. 5f. The optimized design of the short beam example under refined finite element mesh (240 × 120) with $\bar{V} = 0.3$, $\underline{d} = 4.5 \times \min(\Delta x, \Delta y)$ and $\bar{d} = 10.5 \times \min(\Delta x, \Delta y)$, respectively.

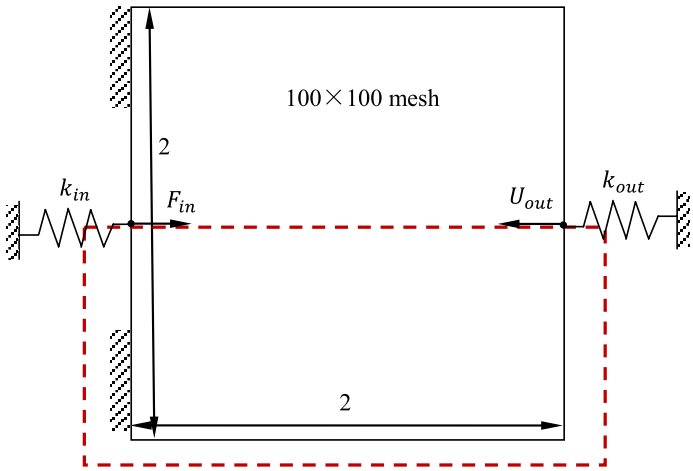

Fig. 6a. The design domain of the compliant mechanism example.

Fig. 6b. The optimized design of the compliant mechanism without length scale control.

order to obtain optimized compliant mechanism without hinge, we can introduce minimum length scale constraint into the problem formulation. Figs. 6c and 6d show the optimized topologies and the corresponding structural skeletons when $\underline{d} = 5 \times \min(\Delta x, \Delta y)$, $\underline{d} = 7 \times \min(\Delta x, \Delta y)$, respectively. From these figures, it can be seen clearly that the hinge does have been eliminated due to the existence of minimum length scale constraint. Although the GA measure of the optimized structure is degenerated (see Table 2 for reference), the risk of damage and fatigue of the resulting compliant mechanism at the hinge point can also be reduced. This is very helpful to guarantee the reliability of the optimal structure.

5.3. Heat conduction example

As pointed out in the previous subsection, the present length scale control measure is pure geometric in nature and is independent on the physics of the problem. It can also be applied to non-structural topology optimization

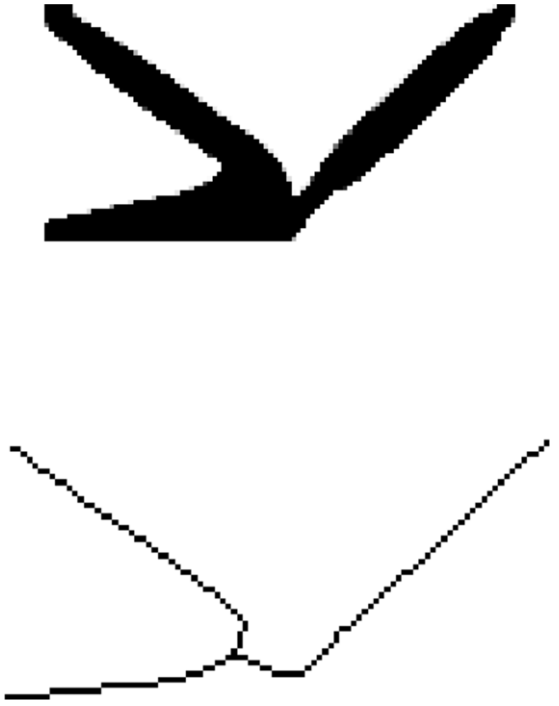

Fig. 6c. The optimized design of the compliant mechanism with length scale control and the corresponding structural skeleton ($\bar{V} = 0.3$ and $\underline{d} = 5 \times \min(\Delta x, \Delta y)$).

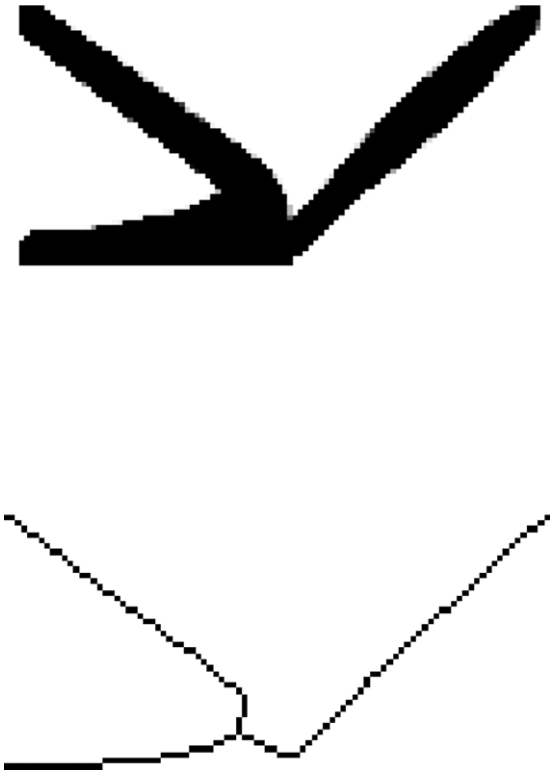

Fig. 6d. The optimized design of the compliant mechanism with length scale control and the corresponding structural skeleton ($\bar{V} = 0.3$ and $\underline{d} = 7 \times \min(\Delta x, \Delta y)$).

Table 2
Optimization results for the compliant mechanism problem.

U_{out} $\underline{d} = 0$	U_{out} $\underline{d} = 5 \times \min(\Delta x, \Delta y)$	U_{out} $\underline{d} = 7 \times \min(\Delta x, \Delta y)$	Volume
−0.7901	−0.7690	−0.7430	0.3

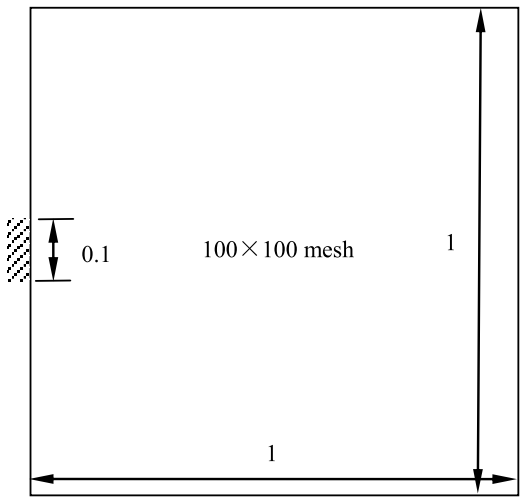

Fig. 7a. The design domain of the heat conduction example.

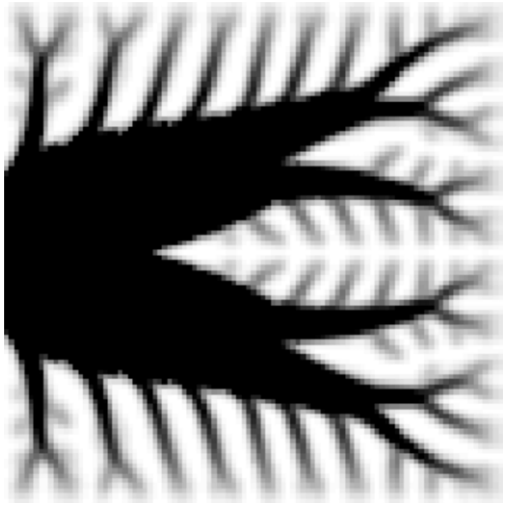

Fig. 7b. The optimized design of the heat conduction problem without length scale control.

problems. To illustrate this point more explicitly, the heat conduction problem shown in Fig. 7a, where the objective is to maximize the heat transfer capacity, is examined under minimum length scale control constraint. We refer the readers to [26] for a more detailed description of this problem. The design domain where distributed unit thermal loading uniformly applied is discretized with a 100 × 100 FEM mesh and the temperature of left-middle side is set to 0, as shown in Fig. 7a. It is worth noting that since the problem under consideration has the gray elements naturally, the original filter form is utilized for obtaining the mesh-independent results. When the upper bound of the available solid material volume is $\bar{V} = 0.5$, the optimized structure without length scale constraints is shown in Fig. 7b. It can

Fig. 7c. The optimized design of the heat conduction problem with length scale control and the corresponding structural skeleton ($\bar{V} = 0.3$ and $\bar{d} = 7 \times \min(\Delta x, \Delta y)$).

be seen that this optimal design is unfavorable for manufacturing due to the existence of a large number of fins with small thickness.

Next, the same problem is reconsidered with length scale constraint being taken into consideration. It is required that the minimum length scale of the thermal fins should be greater than $\underline{d} = 7 \times \min(\Delta x, \Delta y)$. The optimized design and the corresponding structural skeleton are shown in Fig. 7c. From Fig. 7c, it can be seen that compared with the design shown in Fig. 7b, several main heat transfer paths are still retained in the optimal design subjected to length scale constraint. However, the fins with small widths have been eliminated. The optimal design shown in Fig. 7c is more reasonable from manufacturability point of view. Accordingly, the value of the objective function has been decreased from 186.63 to 133.35, due to the existence of length scale constraint.

6. Concluding remarks

In the present paper, a novel approach for explicit and local control of both minimum/maximum length scales in topology optimization of continuum structures is proposed. Our method is established based on the concept of structural skeleton, which has been well addressed in the field of image processing. Once the structural skeleton is identified, the minimum/maximum length scales can be measured accurately, which is the basis to formulate the corresponding functions in a mathematical rigorous way. Numerical examples demonstrate that the proposed approach does have the capability to give a complete control of the length scales of structural features in an explicit and local way. Although mainly structural optimization problems are considered in the present paper, the same idea and the corresponding implementation techniques can also be applied to other multi-disciplinary topology optimization problems. Research results along these directions will be reported elsewhere.

Acknowledgments

We would like to thank Prof. Ole Sigmund from Technical University of Denmark for valuable discussions and suggestions on this paper. The financial supports from the National Natural Science Foundation (10925209, 91216201, 11372004, 11402048), China Postdoctoral Science Foundation (2014M561221), 973 Project of China (2010CB832703), Program for Changjiang Scholars, Innovative Research Team in University (PCSIRT) and 111 Project (B14013) are also gratefully acknowledged.

References

[1] M.P. Bendsoe, N. Kikuchi, Generating optimal topologies in structural design using a homogenization method, Comput. Method Appl. Mech. Engrg. 71 (1988) 197–224.
[2] H.A. Eschenauer, N. Olhoff, Topology optimization of continuum structures: A review, Appl. Mech. Rev. 54 (2001) 331–390.
[3] M.P. Bendsoe, E. Lund, N. Olhoff, O. Sigmund, Topology optimization-broadening the areas of application, Control Cybernet. 34 (2005) 7–35.
[4] X. Guo, G.D. Cheng, Recent development in structural design and optimization, Acta Mech. Sin. 26 (2010) 807–823.
[5] O. Sigmund, On the design of compliant mechanisms using topology optimization, Mech. Struct. Mach. 25 (1997) 493–524.
[6] J. Petersson, O. Sigmund, Slope constrained topology optimization, Internet. J. Numer. Methods Engrg. 41 (1998) 1417–1434.
[7] T.A. Poulsen, A new scheme for imposing minimum length scale in topology optimization, Internet. J. Numer. Methods Engrg. 57 (2003) 741–760.
[8] J.K. Guest, J.H. Prevost, T. Belytschko, Achieving minimum length scale in topology optimization using nodal design variables and projection functions, Internet. J. Numer. Methods Engrg. 61 (2004) 238–254.
[9] J.K. Guest, Imposing maximum length scale in topology optimization, Struct. Multidiscip. Optim. 37 (2009) 463–473.
[10] B.L. Zhu, X.M. Zhang, A new level set method for topology optimization of distributed compliant mechanisms, Internet. J. Numer. Methods Engrg. 91 (2012) 843–871.
[11] S.K. Chen, M.Y. Wang, A.Q. Liu, Shape feature control in structural topology optimization, Comput. Aided Des. 40 (2008) 951–962.
[12] J.Z. Luo, Z. Luo, S.K. Chen, L.Y. Tong, M.Y. Wang, A new level set method for systematic design of hinge-free compliant mechanisms, Comput. Method Appl. Mech. Engrg. 198 (2008) 318–331.
[13] X. Guo, W.S. Zhang, W.L. Zhong, Explicit feature control in structural topology optimization via level set method, Comput. Method Appl. Mech. Engrg. 272 (2014) 354–378.
[14] Y.Y. Kim, G.H. Yoon, Multi-resolution multi-scale topology optimization-a new paradigm, Int. J. Solids Struct. 37 (2000) 5529–5559.
[15] T.A. Poulsen, Topology optimization in wavelet space, Internet. J. Numer. Methods Engrg. 53 (2002) 567–582.
[16] F. Wang, B. Lazarov, O. Sigmund, On projection methods, convergence and robust formulations in topology optimization, Struct. Multidiscip. Optim. 43 (2011) 767–784.
[17] X. Guo, W.S. Zhang, L. Zhang, Robust topology optimization considering boundary uncertainties, Comput. Method Appl. Mech. Engrg. 253 (2013) 356–368.
[18] O. Sigmund, Manufacturing tolerant topology optimization, Acta Mech. Sin. 25 (2009) 227–239.
[19] O. Sigmund, K. Maute, Topology optimization approaches, Struct. Multidiscip. Optim. 48 (2013) 1031–1055.
[20] O. Aichholzer, F. Aurenhammer, D. Alberts, B. Gärtner, A novel type of skeleton for polygons, J. Univ. Comput. Sci. 1 (1995) 752–761.
[21] N. Otsu, A threshold selection method from gray-level histograms, IEEE Trans. Syst. Man Cybern. 9 (1979) 62–66.
[22] A. Rosenfeld, L.S. Davis, A note on thinning, IEEE Trans. Syst. Man Cybern. 25 (1976) 226–228.
[23] F. Petr, O. Stepan, Straight skeleton implementation. In spring conference on computer graphics, Lazlo Szimay-Kalos (1998) 210–218.
[24] C. Arcelli, G. Sanniti di Baja, On the sequential approach to medial line transformation, IEEE Trans. Syst. Man Cybern. 8 (1978) 139–144.
[25] K. Svanberg, The method of moving asymptotes-a new method for structural optimization, Internet. J. Numer. Methods Engrg. 24 (1987) 359–373.
[26] M.P. Bendsoe, O. Sigmund, Topology Optimization-Theory, Method and Applications, Springer, Berlin, 2003.